Journal of Cardiovascular Computed Tomography 13 (2019) 163–169

Contents lists available at ScienceDirect

Journal of Cardiovascular Computed Tomography

journal homepage: www.elsevier.com/locate/jcct

Research paper

Machine-learning integration of CT histogram analysis to evaluate the composition of atherosclerotic plaques: Validation with IB-IVUS

Takanori Masuda[a,e], Takeshi Nakaura[c,*], Yoshinori Funama[d], Tomokazu Okimoto[f], Tomoyasu Sato[b], Toru Higaki[e], Noritaka Noda[a], Naoyuki Imada[a], Yasutaka Baba[e], Kazuo Awai[e]

[a] Department of Radiological Technology, Tsuchiya General Hospital, Nakajima-cho 3-30, Naka-ku, Hiroshima, 730-8655, Japan
[b] Department of Diagnostic Radiology, Tsuchiya General Hospital, Nakajima-cho 3-30, Naka-ku, Hiroshima, 730-8655, Japan
[c] Department of Diagnostic Radiology, Graduate School of Medical Sciences, Kumamoto University, 1-1-1 Honjo, Kumamoto, 860-8556, Japan
[d] Department of Medical Physics, Faculty of Life Sciences, Kumamoto University, Kumamoto, Japan
[e] Department of Diagnostic Radiology, Graduate School of Biomedical Sciences, Hiroshima University, Hiroshima, Japan
[f] Department of Cardiovascular Internal Medicine, Tsuchiya General Hospital, Nakajima-cho 3-30, Naka-ku, Hiroshima, 730-8655, Japan

ARTICLE INFO

Keywords:
Machine learning
Coronary plaque
Coronary CT angiography
Extreme gradient boosting (XGBoost)
Integrated backscatter intravascular ultrasound (IB-IVUS)

ABSTRACT

Background: To determine whether machine learning with histogram analysis of coronary CT angiography (CCTA) yields higher diagnostic performance for coronary plaque characterization than the conventional cut-off method using the median CT number.

Methods: We included 78 patients with 78 coronary plaques who had undergone CCTA and integrated backscatter intravascular ultrasound (IB-IVUS) studies. IB-IVUS diagnosed 32 as fibrous- and 46 as fatty or fibro-fatty plaques. We recorded the coronary CT number and 7 histogram parameters (minimum and mean value, standard deviation (SD), maximum value, skewness, kurtosis, and entropy) of the plaque CT number. We also evaluated the importance of each feature using the Gini index which rates the importance of individual features. For calculations we used XGBoost. Using 5-fold cross validation of the plaque CT number, the area under the receiver operating characteristic curve of the machine learning- (extreme gradient boosting) and the conventional cut-off method was compared.

Results: The median CT number was 56.38 Hounsfield units (HU, 8.00–95.90) for fibrous- and 1.15 HU (−35.8–113.30) for fatty- or fibro-fatty plaques. The calculated optimal threshold for the plaque CT number was 36.1 ± 2.8 HU. The highest Gini index was the coronary CT number (0.19) followed by the minimum value (0.17), kurtosis (0.17), entropy (0.14), skewness (0.11), the mean value (0.11), the standard deviation (0.06), and the maximum value (0.05), and energy (0.00). By validation analysis, the machine learning-yielded a significantly higher area under the curve than the conventional method (area under the curve 0.92 and 95%, confidence interval 0.86–0.92 vs 0.83 and 0.75–0.92, p = 0.001).

Conclusion: The machine learning-was superior the conventional cut-off method for coronary plaque characterization using the plaque CT number on CCTA images.

1. Introduction

Coronary computed tomography angiography (CCTA) may improve the efficiency of triage for invasive coronary angiography (ICA) and reduce radiation exposure.[1] Despite its specific limitations, CT yields valuable information that renders it a potentially useful technique for the early identification and characterization of coronary plaques.[2–5] In coronary imaging, the ultimate goal is to identify individuals at increased risk for acute coronary syndromes (ACS).[6,7] Because ACS are often the first manifestation of disease in previously asymptomatic individuals, early identification of patients at risk for plaque rupture has become an important goal in primary prevention.

The mean CT number is useful for the characterization of coronary plaques.[8–11] Motoyama et al.[12] sub-classified noncalcified plaques into those with a lipid core (cutoff point lower than 30 HU) and fibrous plaques (30–150 HU). To differentiate between fatty- and fibro-fatty plaques we applied 36 ± 3 HU as the optimal CT number threshold. However, the criteria applied to characterize non-calcified plaques

* Corresponding author. Department of Diagnostic Radiology, Graduate School of Medical Sciences, Kumamoto University, 1-1-1 Honjo, Kumamoto 860-8556, Japan. Tel. : +81 096 373 5261; fax: +81 096 373 5342.
E-mail addresses: kff00712@nifty.com, hosyasen@kumamoto-u.ac.jp (T. Nakaura).

https://doi.org/10.1016/j.jcct.2018.10.018
Received 15 February 2018; Received in revised form 2 July 2018; Accepted 19 October 2018
Available online 21 October 2018

Abbreviations

CCTA	coronary CT angiography
IB-IVUS	integrated backscatter intravascular ultrasound
SD	standard deviation
XGBoost	extreme Gradient Boosting
ICA	invasive coronary angiography
ACS	acute coronary syndromes
FOV	field of view
CM	contrast medium
TBW	total body weight
ROI	region of interest
AUC	area under the curve
ROC	receiver operating characteristic

based on CT attenuation are non-uniform due to differences in the examination type, the vessels of interest, and the CT scanning parameters.[13] Also, plaque attenuation on CT angiography (CTA) images is strongly affected by the lumen attenuation.[14] Therefore, generalized plaque CT number may not be sufficiently reliable for clinical use.

The image histogram is a set of metrics calculated by mathematical analysis of digital images; its combination with machine learning has been reported to be of high diagnostic performance for the differentiation of malignant tumors.[15,16] However, it is unknown whether histogram analysis combined with machine learning is useful for the characterization of coronary plaques. To determine whether the evaluation of coronary plaques by machine learning is diagnostically superior to evaluation based on the median CT number we compared the performance of machine learning combined with histogram analysis with the performance of the conventional CT cut-off method.

2. Methods

This retrospective study was approved by our institutional review board; informed consent was waived.

2.1. Patients

Between May 2011 and January 2015, we enrolled 115 consecutive patients who underwent both CCTA and integrated backscatter intravascular ultrasound (IB-IVUS). All presented with moderate stenosis whose calcification did not preclude quantitative assessment by IVUS or CCTA and none harbored side branches between the proximal and distal portions of the lesion. The plaques analyzed in this study were located at least 20 mm from the lesion targeted for intervention. Excluded were patients with unstable angina or myocardial infarction within the previous three months (n = 7) or calcified plaques (n = 30). Therefore, the final study population consisted of 78 patients with right coronary artery (n = 25)-, left main trunk (n = 2)-, left anterior descending branch (n = 39)-, and left circumflex branch (n = 12) plaques. Tissue characterization was performed within two weeks of CCTA using IB-IVUS (IB-IVUS, YD Co., Ltd., Nara, Japan).

2.2. IB-IVUS

Conventional IVUS images and IB signals were acquired at end-diastole using the IVUS imaging system. We used a 40-MHz IVUS catheter (Atlantis; Boston Scientific, Natick, MA); a personal computer equipped with custom software (IBIVUS; YD, Nara, Japan) was connected to the IVUS imaging system. The tip of the IVUS catheter was placed in the coronary vessel with a diameter of at least 2.5 mm. The catheter was then pulled back automatically at a rate of 0.5 mm/s. The radiofrequency signals were acquired of the ECG after the detection of a regular R-R interval. Off-line calculation of the IB values for the acquired radiofrequency signals was performed by retrieval of the stored data. The IB values for each histological category were determined as described previously.[17] Each data set was stored digitally and assessed by a cardiologist blinded to the CT results.

A technician selected a distal branch site as the starting point for analysis. Every 60th image, representing cross-sections exactly 1.0 mm apart, was analyzed. IVUS measurements were performed in accordance with the standards of the American College of Cardiology.[18] Atherosclerotic plaques were defined as at least 0.5-mm-thick structures located between the media and the intima. The plaque volume of each 1-mm section was determined by calculating the maximum plaque area. The vessel plaque burden was calculated by adding the plaque volumes of all sections. To construct IB color-coded maps we divided the mean calibrated IB values for each region of interest (ROI) into four categories where −73 to −63 = fatty, −62 to −55 = fibro-fatty, −54 to −31 = fibrous, and −30 to −23 = calcified.[17] Two-dimensional color-coded maps of the tissue characteristics were analyzed based on these categories.

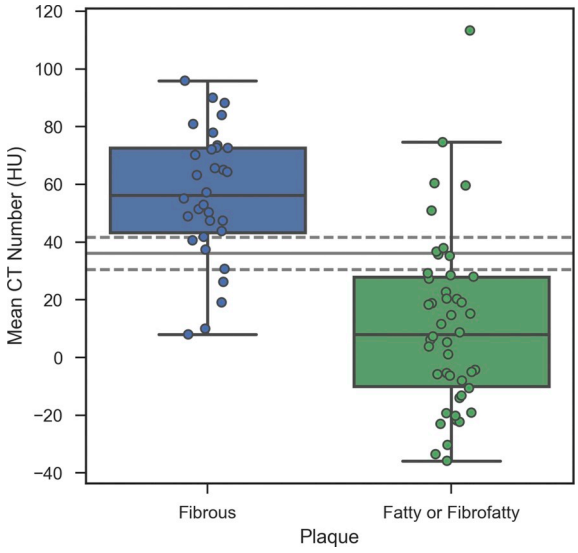

Fig. 1. Box plot of the mean CT number of fibrous and fatty/fibro-fatty plaques. The median CT number was 56.38 HU (8.00–95.90) for fibrous- and 1.15 HU (−35.8–113.30) for fatty or fibro-fatty plaques. There was a significant difference between fibrous- and fatty or fibro-fatty plaques ($p < 0.01$).

Table 1
Summary of the histogram parameters of the fatty- or fibro-fatty plaques.

	Fibrous plaque	Fatty or fibro-fatty plaque	P value
Coronary CT number	279.36 ± 68.52	284.3 ± 64.4	0.75
Kurtosis	3.08 ± 0.95	2.87 ± 0.63	0.29
Minimum value	−30.56 ± 22.57	−67.71 ± 34.35	0.0000002
Entropy	1.92 ± 0.12	1.96 ± 0.12	0.24
Skewness	0.21 ± 0.57	0.27 ± 0.49	0.63
Mean value	56.38 ± 22.57	11.15 ± 30.12	0.0000000001
Standard value	39.39 ± 12.00	115.24 ± 48.81	0.94
Maximum value	161.78 ± 53.16	39.18 ± 13.44	0.0002
Energy	0.01 ± 0.01	0.01 ± 0.01	0.61

2.3. CT scanning and contrast injection protocols

All patients were scanned on a 64-detector row CT scanner (Lightspeed VCT; GE Healthcare, Milwaukee, WI); prospective ECG-

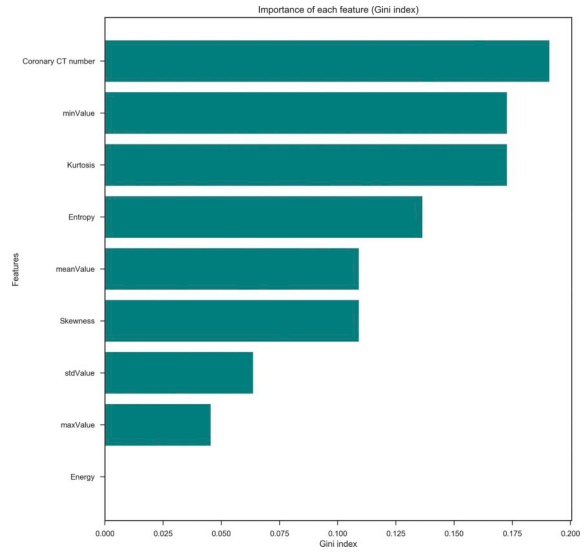

Fig. 2. Bar graph of the Gini index of XGBoost to differentiate between fibrous and fatty/fibro-fatty plaques. The highest Gini index was the coronary CT number (0.19) followed by the minimum value (0.17), kurtosis (0.17), entropy (0.14), skewness (0.11), the mean value (0.11), the standard deviation (0.06), the maximum value (0.05), and energy (0.00).

triggered axial scans were acquired. The CT scanning parameters were 0.35-sec rotation, 0.625-mm detector row width, 0.2 helical pitch (beam pitch), 8.0 mm table movement, 50-cm scan field of view (FOV), 120 kVp, and 400–770 mA. All scans were from the top of the left atrial appendage to the level of the inferior margin of the cardiac apex in the craniocaudal direction. All patients were able to perform breath-holds during the examination. Image reconstruction was in a 15- to 20-cm display FOV depending on the patient body size. Each patient was given nitroglycerin sublingually (0.3 mg) 5 min before scanning. Patients whose heart rate exceeded 65 beats per min after its administration additionally received landiolol hydrochloride (Corebeta; Ono, Osaka, Japan). We injected the contrast medium (CM, Iomeron 350; Eisai, Tokyo, Japan) through a 20-gauge catheter into the antecubital vein using a power injector (Dual Shot; Nemoto-Kyorindo, Tokyo, Japan). We used the test bolus scan to obtain the scan delay for CCTA. The injection volume was total body weight (TBW) × 0.6 ml, administered during 12 s. As the CM for the test bolus was diluted (30% CM, 70% saline), the CM volume was TBW × 0.18 ml (TBW × 0.6 ml × 30%). CM delivery was followed by flushing with 20 ml of physiological saline at the same injection rate.

2.4. Histogram, histogram features and machine learning

For computation of the histogram features, Digital Imaging and Communications in Medicine images of the 78 plaques were imported to the software package LIFEx (version 2.00, http://www.lifexsoft.org/). We manually selected the region of interest (ROI) of plaques on axial or cross-section multiplanar reformation images to calculate the histogram features, the ROI greater than 1.0 mm^2 was placed on at least 4 randomly selected points within each plaque.

We built machine learning classifiers that applied extreme Gradient Boosting (XGBoost) using Python (version 3.5; https://www.python.org/) and scikit-learn (version 0.18.1, http://scikit-learn.org/stable/) to discriminate among fibrous-, fatty-, and fibro-fatty plaques. We performed optimization by using the Python scikit-learn cross-validation function. The applied parameters were:

XGB Classifier: (base_score = 0.5, booster = 'gbtree', colsample_bylevel = 1, colsample_bytree = 0.597959992516703, gamma = 0, learning_rate = 1.0, max_delta_step = 0, max_depth = 8, min_child_weight = 1, missing = none, n_estimators = 100, n_jobs = 1, nthread = none, objective = 'binary:logistic', random_state = 0, reg_alpha = 0, reg_lambda = 1, scale_pos_weight = 1, seed = none, silent = true, subsample = 0.8298276978060357).

For coronary plaque classification we recorded the CT number on CCTA images and 7 histogram parameters (minimum value, mean value, standard deviation (SD), maximum value, skewness, kurtosis, and entropy). We used histograms because the plaque volume was small and the size of many plaques could not be measured. As did Berenguer et al.,[19] we found that many parameters are not required. There is severe overlap in each feature; however, XGBoost using multi-variate features barely classified the composition of coronary plaques by the combination of many features. We performed simple normalization by first calculating the mean and the standard deviation for each feature. Then we subtracted the mean from each feature and divided the obtained result by the standard deviation. We trained the machine learning classifiers on fibrous- and fatty or fibro-fatty plaques by applying a 5-fold cross-validation method to separate the training from the testing of the discriminant by classifiers.[20] The cross-validation function of scikit-learn automatically separated the population into 5-folds cross-validation. The parameters of XGBoost were selected by a grid search method. To evaluate the importance of individual features we calculated the Gini index using XGBoost.[21]

As a control we also built conventional CT-number-based classifiers by calculating the threshold of the CT number to differentiate among fibrous-, fatty-, and fibro-fatty plaques.

2.5. Statistical analysis

Statistical analyses were performed with the free Python programing software (version 3.5; https://www.python.org/). We compared the coronary CT number and the 7 histogram parameters applied to the coronary plaques on CCTA images using the Wilcoxon rank sum test.

The area under the curve (AUC) of our receiver operating characteristic (ROC) analysis of machine learning and conventional CT-number-based classifiers was calculated. We compared the diagnostic performances of the AUC obtained with machine learning and with the conventional CT-number-based method using the DeLong test. A p value < 0.05 was considered to indicate a statistically significant difference. We also calculated the importance of all features using XGBoosting.

3. Results

We sampled 78 ROIs on CT images that corresponded with defined tissue types on IB-IVUS (32 fibrous-, 46 fatty or fibro-fatty plaque, 78 lumens).

The median CT number was 56 HU (8–96) for fibrous- and 1 HU (−36 to 113) for fatty or fibro-fatty plaques ($p < 0.01$, Fig. 1). The calculated optimal threshold for the plaque CT number was 36 ± 3 HU.

A summary of the histogram parameters of the 78 fatty- or fibro-fatty plaques is shown in Table 1. There was a significant difference in their mean-, maximum-, and minimum values. The coronary CT number (0.19) exhibited the highest Gini index for all parameters, followed by the minimum value (0.17), kurtosis (0.17), entropy (0.14), skewness (0.11), the mean- (0.11), standard- (0.06), and maximum value (0.05), and energy (0.00) (Fig. 2).

The 2D decision boundaries of XGBoost involved 2 dimensions for the 4 most important parameters, i.e. the coronary CT number, minimum value, kurtosis, and entropy, although 9 dimensions were actually used. There were large overlaps in most features; XGBoost suboptimally classified the composition of coronary plaques when multiple features were applied (Fig. 3).

The AUC and the 95% CI were 0.92 and 0.86–0.92 for the machine learning- and 0.83 and 0.75–0.92 for the conventional CT number-

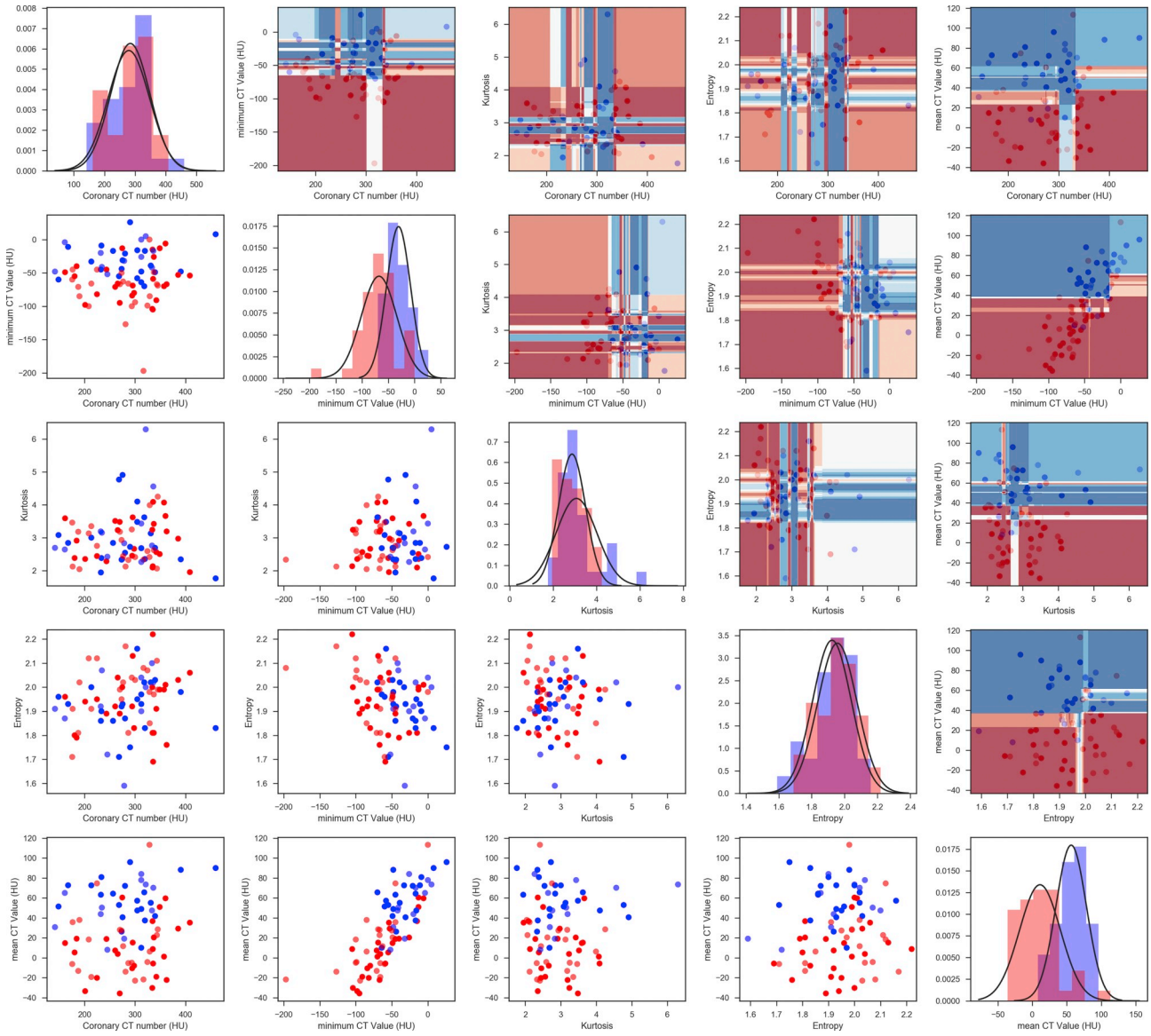

Fig. 3. 2D decision boundaries of XGBoost with two dimensions for the 4 most important parameters. Red and blue markers identify mean fatty or fibro-fatty plaques, and mean fibrous plaques, respectively. Lines indicate the probability of the XGBoost classifier. There is severe overlap in all features; however, XGBoost barely classified the composition of coronary plaques. (For interpretation of the references to color in this figure legend, the reader is referred to the Web version of this article.)

based method. Validation analysis showed that the machine-learning-yielded a significantly higher AUC than the conventional method ($p = 0.001$) (see Figs. 4–6).

4. Discussion

Our study suggests that with respect to the characterization of coronary plaques, the diagnostic performance of machine learning using histogram parameters is significantly higher than of the conventional cut-off method using the plaque CT number on CCTA images.

There are many reports that suggested that the CT number depending on the plaque compornents such as calcified-, noncalcified-(soft), and mixed plaques.[12,22–24] We applied 36 ± 3 HU as the optimal CT number threshold to differentiate between fatty- and fibro-fatty plaques. Although CCTA is a promising tool for the characterization of atherosclerotic coronary lesions, we suggest that for the assessment of such plaques, machine learning is superior to the conventional method that uses the mean CT number.

The differentiation between lipid rich and fibrous lesions represents a major challenge for non-invasive imaging. Some studies suggest that higher attenuation plaques correspond to predominantly fibrous plaques and plaques with less than 30 HU density showed a good correlation with virtual histology intravascular ultrasound lipid rich plaques.[2,25] The presence of positive remodeling and low-attenuation plaques on coronary CTA was associated with higher risk of developing ACS.[4] Low attenuation plaques (> 30 HU) were more prevalent in patients presenting with ACS than with stable angina pectoris.[12] It has been shown to possess a high predictive value in predicting future cardiac events and is considered one of the imaging correlates of an unstable plaque.

To our knowledge, this is the first clinical study to evaluate coronary plaque components by machine-learning integration of CT histogram analysis. Based on their phantom study, Didem et al.[26] reported that machine learning using virtual monochromatic images for dual-energy CT was useful to classify fibrous and lipid plaques. However, dual-energy CT is not widely used for coronary CT angiography. We suggest the method we propose, i.e. machine-learning integration of single CT histogram analysis, is practical for clinical examinations.

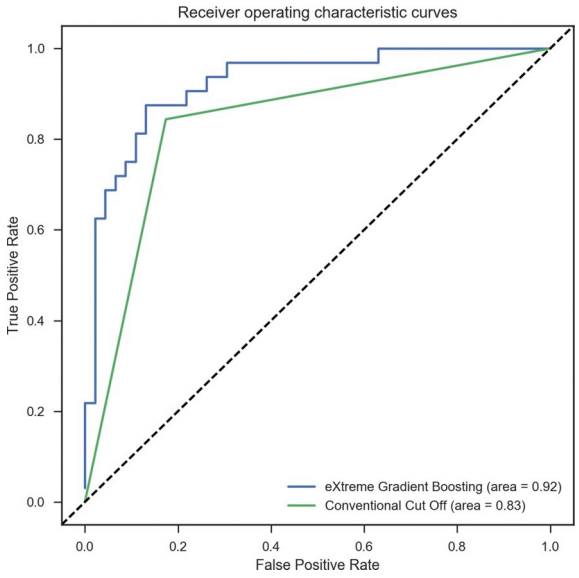

Fig. 4. ROC curves of the machine learning method and the conventional CT number-based method. Validation analysis showed that the AUC for the machine learning- and the conventional CT-number-based method was 0.92 and 0.83, respectively (p = 0.01).

Our study suggested that the machine learning using CT number histogram might be useful to the characterization of coronary plaques during CCTA. Image histograms are a set of metrics calculated from digital images based on mathematical analysis. Histogram analysis was of high diagnostic value with respect to brain-,[15] skin-,[27] prostate-,[16] and lung cancers.[28,29]

The Gini index and XGBoost suggests that the CT number of the coronary artery lumen plays an important role for machine learning to differentiate among fatty- and fibro-fatty coronary artery plaques. Others[8,14] reported that the higher the lumen attenuation, the higher was the plaque attenuation. As intravascular attenuation significantly affects attenuation of coronary atherosclerotic plaques assessed on CCTA images, care must be taken when plaque characterization is based on absolute attenuation values. Because machine learning includes information on coronary artery attenuation, the resultant AUC was significantly higher than that obtained with the conventional method.

Some study limitations must be addressed. First, this is a small single-center-, single-protocol study and only the performance of the machine-learning algorithm was evaluated. The clinical implications of our findings remain unclear and require the integration of machine-learning models into image analysis software. Secondly, as our sample size was relatively small, additional analysis such as high-level texture analysis or sub-analysis based on the patient gender, body mass index, and heart rate was not possible. Also, we did not compare our acquisition method with CTA obtained with other protocols. Thirdly, we did not make attenuation adjustments for proximal or distal plaques. Fourthly, findings are limited to moderate stenoses in a narrowly-defined patient population at very specific locations. Partially calcified plaques are not mentioned. Only non-calcified lesions were included in this analysis. Lastly, we used only the CT number to define the plaques and did not test ML against previously reported plaque analysis software.

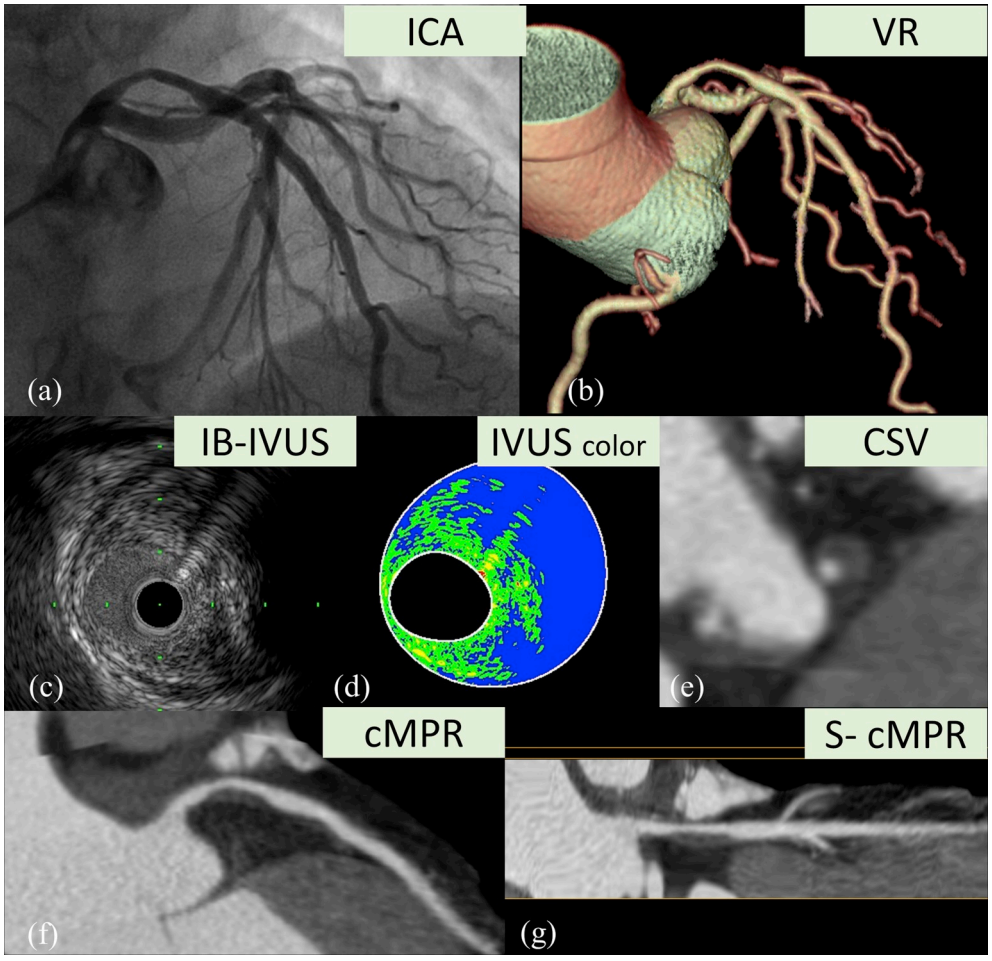

Fig. 5. A 77-year-old man with ischemic heart disease. X-ray angiography (a), volume-rendering image of CTA (b), IB-IVUS image (c), IVUS color image (d), short axis image (e), curved multi-planner image (f), and stretched curved multi-planner image (g). IB-IVUS suggested a fatty plaque. However, the mean CT number of this plaque is 50.9 HU, and conventional CT number threshold method concluded that it might be fibrous plaque. On the other hand, machine learning suggested that it might be fatty or fibro-fatty plaque (probability 94.2%). The relatively high intra-coronary attenuation (348.9 HU) has the possibility to influence the diagnostic ability of the conventional method. (For interpretation of the references to color in this figure legend, the reader is referred to the Web version of this article.)

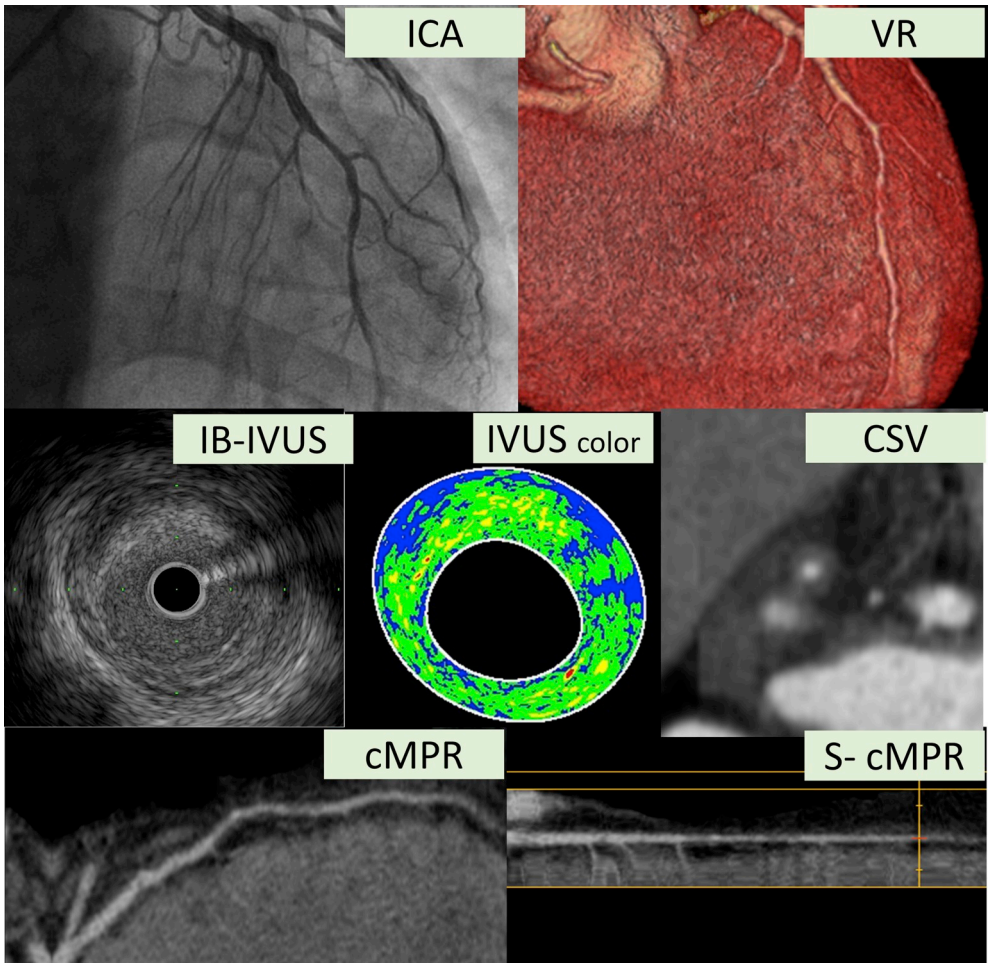

Fig. 6. A 67-year-old man with stable angina pectoris. X-ray angiography (a), volume-rendering image of CTA (b), IB-IVUS image (c), IVUS color image (d), short axis image (e), curved multi-planner image (f), and stretched curved multi-planner image (g). IB-IVUS suggested a fibrous plaque. However, the mean CT number of this plaque is 30.7 HU, and conventional CT number threshold method concluded that it might be fatty or fibro-fatty plaque. On the other hand, machine learning suggested that it might be fibrous plaque (probability 57.0%). The relatively low intra-coronary attenuation (141.4 HU) has the possibility to influence the diagnostic ability of the conventional method. (For interpretation of the references to color in this figure legend, the reader is referred to the Web version of this article.)

5. Conclusion

In conclusion, for coronary plaque characterization, the diagnostic performance of machine learning was superior to the conventional cut-off method using the plaque CT number on CCTA images.

Disclosures

The authors have no conflicts of interest directly relevant to the content of this article.

References

1. Douglas PS, Pontone G, Hlatky MA, et al. Clinical outcomes of fractional flow reserve by computed tomographic angiography-guided diagnostic strategies vs. usual care in patients with suspected coronary artery disease: the prospective longitudinal trial of FFR(CT): outcome and resource impacts study. *Eur Heart J.* 2015;36:3359–3367.
2. Marwan M, Taher MA, El Meniawy K, et al. In vivo CT detection of lipid-rich coronary artery atherosclerotic plaques using quantitative histogram analysis: a head to head comparison with IVUS. *Atherosclerosis.* 2011;215:110–115.
3. Schlett CL, Maurovich-Horvat P, Ferencik M, et al. Histogram analysis of lipid-core plaques in coronary computed tomographic angiography: ex vivo validation against histology. *Invest Radiol.* 2013;48:646–653.
4. Motoyama S, Sarai M, Harigaya H, et al. Computed tomographic angiography characteristics of atherosclerotic plaques subsequently resulting in acute coronary syndrome. *J Am Coll Cardiol.* 2009;54:49–57.
5. Henzler T, Porubsky S, Kayed H, et al. Attenuation-based characterization of coronary atherosclerotic plaque: comparison of dual source and dual energy CT with single-source CT and histopathology. *Eur J Radiol.* 2011;80:54–59.
6. Non-invasive cardiac imaging technologies for the diagnosis of coronary artery disease: a summary of evidence-based analyses. *Ont Health Technol Assess Ser.* 2010;10:1–40.
7. Lloyd-Jones D, Adams RJ, Brown TM, et al. Heart disease and stroke statistics–2010 update: a report from the American Heart Association. *Circulation.* 2010;121:e46–e215.
8. Cademartiri F, Mollet NR, Runza G, et al. Influence of intracoronary attenuation on coronary plaque measurements using multislice computed tomography: observations in an ex vivo model of coronary computed tomography angiography. *Eur Radiol.* 2005;15:1426–1431.
9. Ohota M, Kawasaki M, Ismail TF, Hattori K, Serruys PW, Ozaki Y. A histological and clinical comparison of new and conventional integrated backscatter intravascular ultrasound (IB-IVUS). *Circ J.* 2012;76:1678–1686.
10. Sano K, Kawasaki M, Okubo M, et al. In vivo quantitative tissue characterization of angiographically normal coronary lesions and the relation with risk factors: a study using integrated backscatter intravascular ultrasound. *Circ J.* 2005;69:543–549.
11. Nair A, Margolis MP, Kuban BD, Vince DG. Automated coronary plaque characterisation with intravascular ultrasound backscatter: ex vivo validation. *EuroIntervention.* 2007;3:113–120.
12. Motoyama S, Kondo T, Sarai M, et al. Multislice computed tomographic characteristics of coronary lesions in acute coronary syndromes. *J Am Coll Cardiol.* 2007;50:319–326.
13. Kristanto W, van Ooijen PM, Jansen-van der Weide MC, Vliegenthart R, Oudkerk M. A meta analysis and hierarchical classification of HU-based atherosclerotic plaque characterization criteria. *PloS One.* 2013;8.
14. Kidoh M, Utsunomiya D, Oda S, et al. Evaluation of the effect of intracoronary attenuation on coronary plaque measurements using a dual-phase coronary CT angiography technique on a 320-row CT scanner–in vivo validation study. *Acad Radiol.* 2016;23:315–320.
15. Zhang X, Yan LF, Hu YC, et al. Optimizing a machine learning based glioma grading system using multi-parametric MRI histogram and texture features. *Oncotarget.* 2017;8:47816–47830.
16. Gertych A, Ing N, Ma Z, et al. Machine learning approaches to analyze histological images of tissues from radical prostatectomies. *Comput Med Imag Graph.* 2015;2:197–208.
17. Kawasaki M, Takatsu H, Noda T, et al. In vivo quantitative tissue characterization of human coronary arterial plaques by use of integrated backscatter intravascular ultrasound and comparison with angioscopic findings. *Circulation.* 2002;105:2487–2492.
18. Mintz GS, Nissen SE, Anderson WD, et al. American College of cardiology clinical expert consensus document on standards for acquisition, measurement and reporting of intravascular ultrasound studies (IVUS). A report of the american College of cardiology task force on clinical expert consensus documents. *J Am Coll Cardiol.*

2001;37:1478–1492.
19. Berenguer R, Pastor-Juan MDR, Canales-Vázquez J, et al. Radiomics of CT features may Be nonreproducible and redundant: influence of CT acquisition parameters. *Radiology.* 2018 Apr 24:172361.
20. Sano K, Kawasaki M, Ishihara Y, et al. Assessment of vulnerable plaques causing acute coronary syndrome using integrated backscatter intravascular ultrasound. *J Am Coll Cardiol.* 2006;47:734–741.
21. Relative Importance of Predictor Variables" of the Book the Elements of StatisticalLearning: Data Mining, Inference, and Prediction, page 367.
22. Schroeder S, Kopp AF, Baumbach A, et al. Noninvasive detection and evaluation of atherosclerotic coronary plaques with multislice computed tomography. *J Am Coll Cardiol.* 2001;37:1430–1435.
23. Tsagakis K, Konorza T, Dohle DS, et al. Hybrid operating room concept for combined diagnostics, intervention and surgery in acute type A dissection. *Eur J Cardio Thorac Surg.* 2013;43:397–404.
24. Hoffmann U, Moselewski F, Nieman K, et al. Noninvasive assessment of plaque morphology and composition in culprit and stable lesions in acute coronary syndrome and stable lesions in stable angina by multidetector computed tomography. *J Am Coll Cardiol.* 2006;47:1655–1662.
25. Narula J, Garg P, Achenbach S, Motoyama S, Virmani R, Strauss HW. Arithmetic of vulnerable plaques for noninvasive imaging. *Nat Clin Pract Cardiovasc Med.* 2008;5.
26. Yamak D, Panse P, Pavlicek W, Boltz T, Akay M. Non-calcified coronary atherosclerotic plaque characterization by dual energy computed tomography. *IEEE J Biomed Health Inform.* 2014;18:939–945.
27. Stanley RJ, Moss RH, Van Stoecker W, Aggarwal C. A fuzzy-based histogram analysis technique for skin lesion discrimination in dermatology clinical images. *Comput Med Imag Graph.* 2003;27:387–396.
28. Adetiba E, Olugbara OO. Lung cancer prediction using neural network ensemble with histogram of oriented gradient genomic features. *ScientificWorldJournal.* 2015;786013:23.
29. Gao X, Chu C, Li Y, et al. The method and efficacy of support vector machine classifiers based on texture features and multi-resolution histogram from (18)F-FDG PET-CT images for the evaluation of mediastinal lymph nodes in patients with lung cancer. *Eur J Radiol.* 2015;84:312–317.